Proceedings of the 6th International Conference on Energy Harvesting, Storage, and Transfer (EHST'22)
Niagara Falls, Canada – June 08-10, 2022
Paper No. 137
DOI: 10.11159/ehst22.137

Solidification Process inside a Novel Toroidal Tube Heat Exchanger

Mohammad Reza Mohaghegh[1], Mehran Bozorgi[2], Kasra Ghasemi[3], Syeda Tasnim[4], Shohel Mahmud[5]
School of Engineering, University of Guelph
Guelph, Ontario, Canada
[1]mohaghem@uoguelph.ca; [2]mbozorgi@uoguelph.ca, [3]kghasemi@uoguelph.ca, [4]stasnim@uoguelph.ca
[5]smahmud@uoguelph.ca

Abstract - Concentric tube and shell and tube latent heat exchangers filled with phase change material (PCM) in the tube part are interesting latent heat thermal energy storage (LHTES) systems that have attracted researchers' attention due to high energy storage density during the charging (melting) and discharging (solidification) processes. Inadequate phase change process reduces the thermal performance of LHTES systems. An effective design can facilitate and accelerate the phase change process. In this study, a novel toroidal shape is proposed for the inner part of the heat exchanger (tube) and the solidification process inside this tube is investigated. A mathematical model based on the enthalpy-porosity approach is developed and numerically solved by finite volume method to simulate the energy transport processes inside the system. The progression of the discharging process is also numerically visualized. Several transient heat transfer characteristics, e.g., thermal filed, solid fraction, average temperature, and energy released during solidification, are determined and depicted.

Keywords**:** PCM, Solidification, Heat exchanger, Toroidal tube, Thermal energy storage.

1. Introduction

Thermal Energy Storage (TES) systems are one of the widely used energy storage systems [1]. TES systems integrated with Phase Change Material (PCM) known as Latent Heat Thermal Energy Storage (LHTES) stand out as the most efficient with most applications due to their high storage density, efficiency, and isothermal behavior during heat storage and release [2]. These unique features also make them suitable for thermal energy management applications as well. However, the inherent low thermal conductivity of most PCMs leads to a weakness in the performance of LHTES systems [3-5].

One of the effective ways to address this issue is the proper geometric design of these systems, as it causes an improvement in discharging power due to accelerating the solidification process [6]. The concentric tube and shell-and-tube latent thermal storage (ST-LHTES) systems are widely used heat exchanger units [7]. The optimized design for such systems significantly affects the performance [8, 9]. Most literature have used concentric tube heat exchangers because of their simplicity in design. However, there are disadvantages such as limitation in length and small heat losses from the outer shell [10].

The literature survey shows a few studies on unconventional designs in heat exchangers to enhance thermal performance, such as the spiral coil tube [11], the helical tube [12], and the flat spiral tube [13]. However, there are still gaps in the existing literature on innovative designs examining their effects on the thermal performance of the LHTES systems. Therefore, there are motivations to work further in this area. Patel et al. [10] suggested innovative toroidal tube heat exchangers. However, they studied the melting process of PCM. Due to the complexity of the solidification process, very limited works have been conducted to investigate solidification, while there are plenty of research works conducting the melting process.

The present study is aimed to investigate the solidification process of PCM inside a toroidal tube of a shell and tube latent heat exchanger. To the best of the authors' knowledge, no attempts have been made to analyze the solidification process inside a toroidal tube latent heat exchanger, and this research is the first of its kind.

2. Physical Model

2.1. Geometry

The three-dimensional and axisymmetric views of a circular toroid tube heat exchanger, along with the main geometry characteristics, are presented in Fig. 1, where r_0 (i.e., minor radius) is the radius of the vertical cross-section surface which is revolutionized around the θ axis at a distance of R_0 (i.e., major radius) to form the toroid shape. The values used for geometric dimensions corresponded to minor and major radii are 30 mm and 120 mm, respectively.

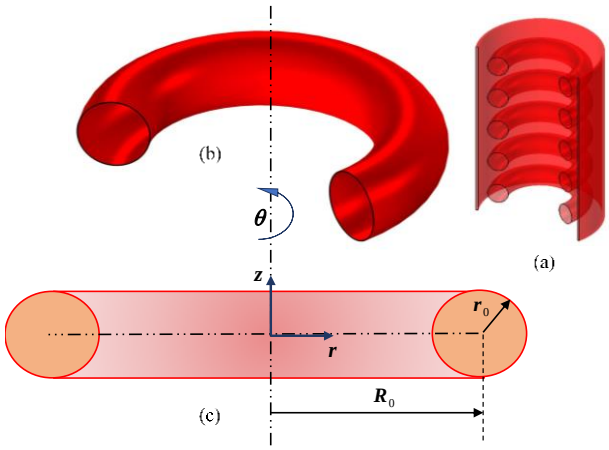

Fig. 1: Schematic diagram of the circular toroid geometry: (a) 3D view of the system, (b) isometric view of the toroidal tube unit, and (c) front sectional view of a unit system.

In the present shell and tube heat exchanger system, the hollow toroidal tube is filled with a bio-based PCM (coconut oil) and is surrounded by a cold heat transfer fluid (HTF) in the shell part. The initial temperature (T_0) of PCM is assumed to be 24°C which is the melting point of PCM, while the lateral wall temperature (T_c) is kept at 14°C, equal to HTF temperature ($T_c = T_{HTF}$).

Different types of PCMs with a wide range of thermophysical properties are available in the market that can be used for different applications. In this work, coconut oil is used as PCM due to some unique properties, i.e., nontoxicity for safe applications such as food industry (as it is edible) [14], melting temperature close to the room temperature, low degree of supercooling [15] and low volumetric thermal expansion [16]. The properties of the coconut oil are measured at the University of Guelph (Advanced Energy Conversion and Control Lab, Bio-Innovation Research Lab, and Food Research Lab) and can be found in [16].

2.2. Mathematical Modeling

The conservation equations of mass, momentum, and energy are formulated as the governing equations in the present model. The influence of natural convection is also taken into account by considering convection terms in the energy equation, which play an important role in the liquid part of the system. In the present modeling, the liquid phase of PCM is considered as a Newtonian incompressible fluid, and flow is laminar. All properties are assumed constant in each phase, except density in the buoyancy term which is estimated by a linear density-temperature relation (the Boussinesq approximation). Having axisymmetric geometry, the problem is simplified to a 2-D axisymmetric model. To model the phase change process, the enthalpy-porosity technique is used [6, 17, 18]. The conservation equations of mass, momentum, and energy are presented as Eqs. (1)-(4):

Conservation of mass:

$$\frac{\partial u}{\partial r} + \frac{u}{r} + \frac{\partial w}{\partial z} = 0 \qquad (1)$$

Conservation of *r*-momentum (radial direction):

$$\rho\left(\frac{\partial u}{\partial t}+u\frac{\partial u}{\partial r}+w\frac{\partial u}{\partial z}\right)=-\frac{\partial p}{\partial r}+\mu\left(\frac{\partial^2 u}{\partial r^2}+\frac{1}{r}\frac{\partial u}{\partial r}-\frac{u}{r^2}+\frac{\partial^2 u}{\partial z^2}\right)+S_r \quad (2)$$

Conservation of z-momentum equation (axial direction):

$$\rho\left(\frac{\partial w}{\partial t}+u\frac{\partial w}{\partial r}+w\frac{\partial w}{\partial z}\right)=-\frac{\partial p}{\partial z}+\mu\left(\frac{\partial^2 w}{\partial r^2}+\frac{1}{r}\frac{\partial w}{\partial r}+\frac{\partial^2 w}{\partial z^2}\right)+\rho g\beta(T-T_m)+S_z \quad (3)$$

Conservation of energy:

$$\rho c_p\left(\frac{\partial T}{\partial t}+u\frac{\partial T}{\partial r}+w\frac{\partial T}{\partial z}\right)=k\left[\frac{1}{r}\frac{\partial}{\partial r}\left(r\frac{\partial T}{\partial r}\right)+\frac{\partial^2 T}{\partial z^2}\right] \quad (4)$$

where u and w represent the components of velocity in the radial (r) and axial (z) directions, respectively. In these equations, also, t, p, g, and T represent time, pressure, gravitational acceleration, and temperature, respectively. Parameters ρ, μ, β, k, c_p and T_m are related to the PCM properties in each phase. During the phase change, a transition occurs between the solid and liquid parts within a small transition temperature interval (mushy region) ΔT_m, which is considered to a reasonable value of 1 °C in this work. Hence, thermophysical properties (η) within different phases or regions (i.e., solid, mushy, and liquid) are approximated as [9]:

$$\eta = f\,\eta_l + (1-f)\,\eta_s \quad (5)$$

where f is the liquid fraction which varies from 0 in solid to 1 in the liquid state as follows [6]:

$$f=\begin{cases}0 & T<T_m\\ \dfrac{T-(T_m-\Delta T_m)}{2\Delta T_m} & T_m\le T\le T_m+\Delta T_m\\ 1 & T>T_m+\Delta T_m\end{cases} \quad (6)$$

The last terms on the right-hand side of the momentum equations (i.e., Eqs. (2) and (3)) are sink terms in the form of the Carman-Koseny equation related to the mushy region. Detailed information on Eqs. (5) to (9) and their terms, can be found in previous works of the present author(s), i.e., Refs. [6] and [9]. The system is considered at the initial temperature T_0 at the start of the heat transfer process. Then, the wall surface of the toroidal tube is suddenly exposed to a lower temperature (HTF temperature; T_h) to initiate the solidification process. No-slip condition for fluid flow field is also applied to the surface. The initial and boundary conditions for all cases are presented in Eq. (8).

$$\begin{aligned}&\text{Initial conditions } (t=0): \; u=w=0,\; T=T_0\\ &\text{Boundary conditions: } u=w=0,\; T=T_h\end{aligned} \quad (8)$$

3. Results and Discussion

The different numerical results driven from simulations are presented in this section. Fig. 2 shows the progression of the solidification process of PCM inside the toroidal tube and corresponding solid fractions values at the different stages of the phase change process. Isothermal floods and solid front lines are used to represent thermal fields and phase change interface in these images, respectively.

The initial state of PCM is in liquid form at the temperature of 24°C (i.e., equal to T_m). The wall surface of the tube is suddenly exposed to a colder environment (HTF). Therefore, thermal energy starts to transfer from the liquid PCM to the cold surface of the toroidal tube. At this stage, a very thin layer of solid PCM attached to the inside surface of the toroidal tube appears, which is formed in a shape similar to the hollow toroidal tube. At the early stages of the solidification process, the viscous force is dominant compared to the buoyancy and inertial forces, the liquid layer remains nearly motionless, and therefore conduction is the dominant heat transfer regime (e.g., 10 s and 100 s). As time advances further, the natural convection effects, formed a boundary layer in the liquid side (t=1000 s and 3000 s). Beyond t=3000 s, conduction is the dominant mode, and the temperature sensibly drops to HTF temperature (shrinking liquid region). Once

the solidification is completed (SF=1 at t=5810 s), heat transfer from relatively colder liquid PCM to the warmer solid PCM will still continue at a slower rate until the temperature of the entire system reaches the cold wall temperature thermal equilibrium state, e.g., t=14000 s). To quantify the solidification process, the solid fraction (SF) is defined by following equation:

$$SF = \frac{\text{Volume of the solid PCM}}{\text{Total (liquid+solid) volume of PCM}} \times 100 \quad (9)$$

The temporal variation of the solid fraction profile during solidification is depicted in Fig 3. As can be seen, towards the end of the solidification, a large upper portion of the system is occupied by cold solid PCM, and the temperature gradients are reduced. Therefore, the rate of solidification slows down. the slope of graphs for both cases at this stage is less steep.

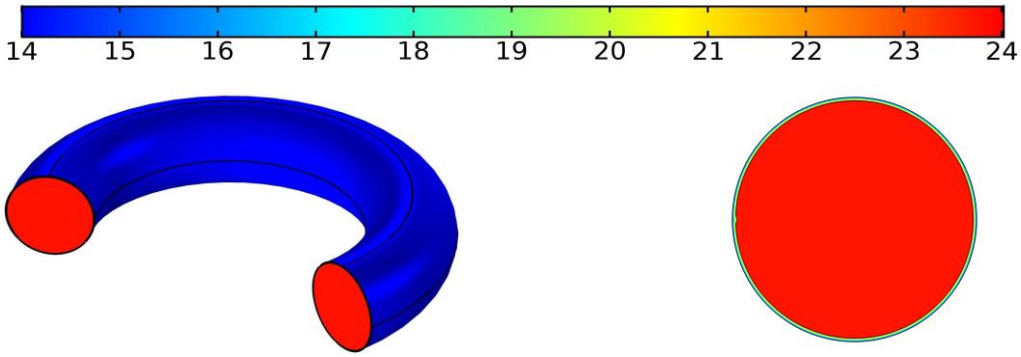

10 s (SF=5.8%)

100 s (SF=16.2%)

1000 s (SF=50.3%)

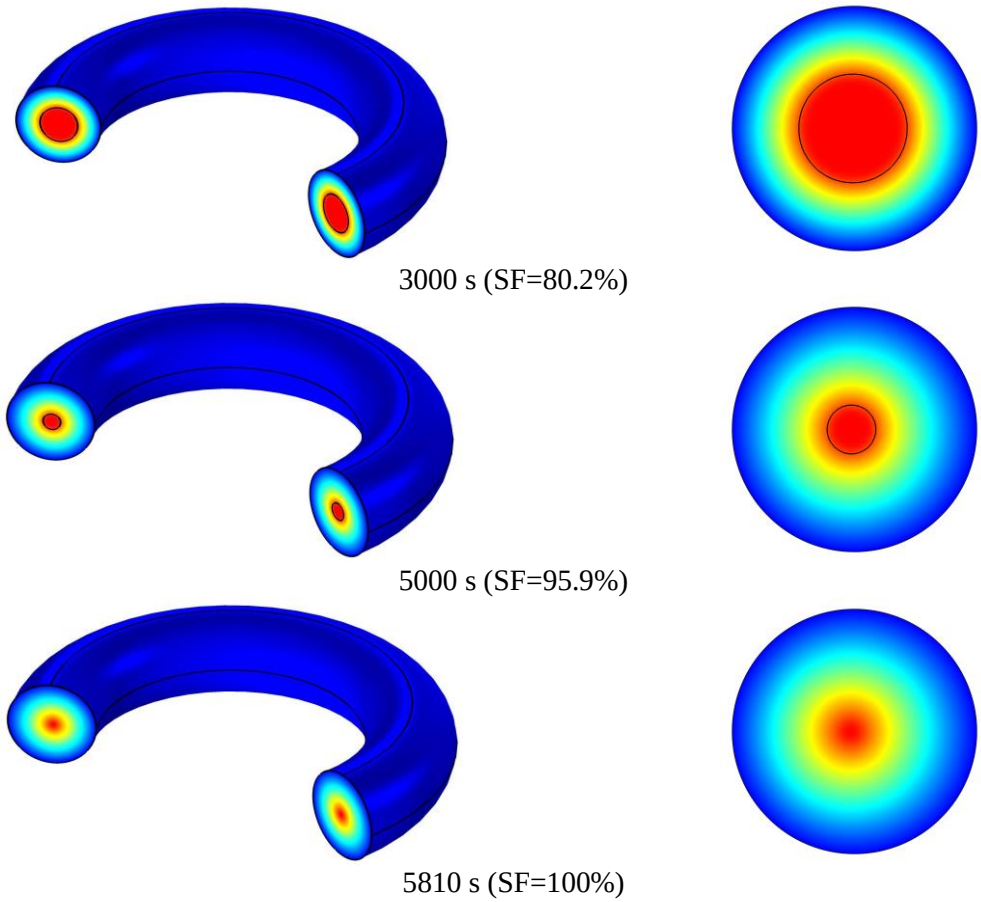

Fig. 2: Progression of the solidification process in the toroidal tube; 3D (left) and 2D (right) views.

The temporal variation of the average PCM temperature is plotted in Fig 4. Being symmetric with respect to θ axis, the T_{ave} can be calculated by the following integration:

$$T_{ave} = \frac{\int_A \mathrm{T}(\mathrm{r}, \mathrm{z})\mathrm{dA}}{\int_A \mathrm{dA}} \qquad (10)$$

where A is the (vertical) cross-sectional area. The general trend in these profiles indicates the three distinct patterns: sharp slope in the temperature profiles in early stages due to high gradient temperature (conduction), continuous growth in temperature with almost uniform slope (convection), and finally, a slow rate in the temperature changes (as a result of decreasing temperature gradients and therefore decreasing heat transfer) to reach the equilibrium state ($T = T_c$).

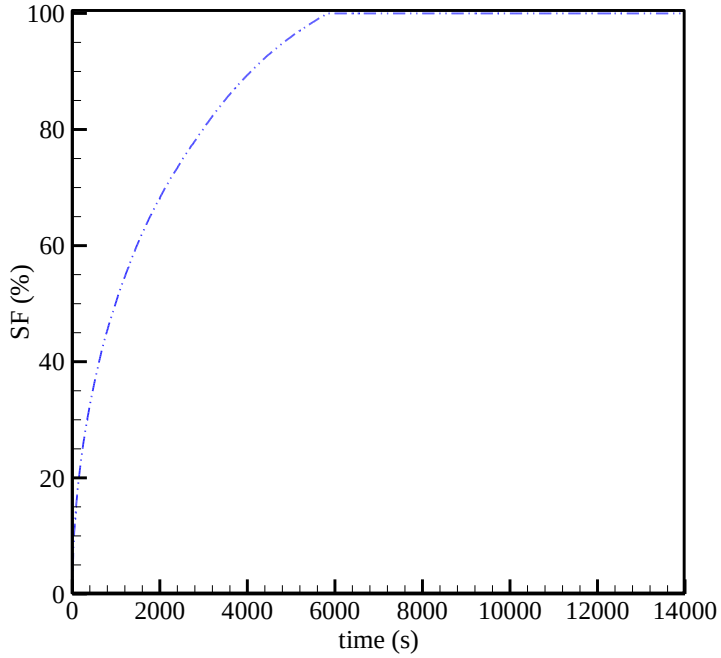

Fig. 3: The temporal variation of solid fraction during phase change process.

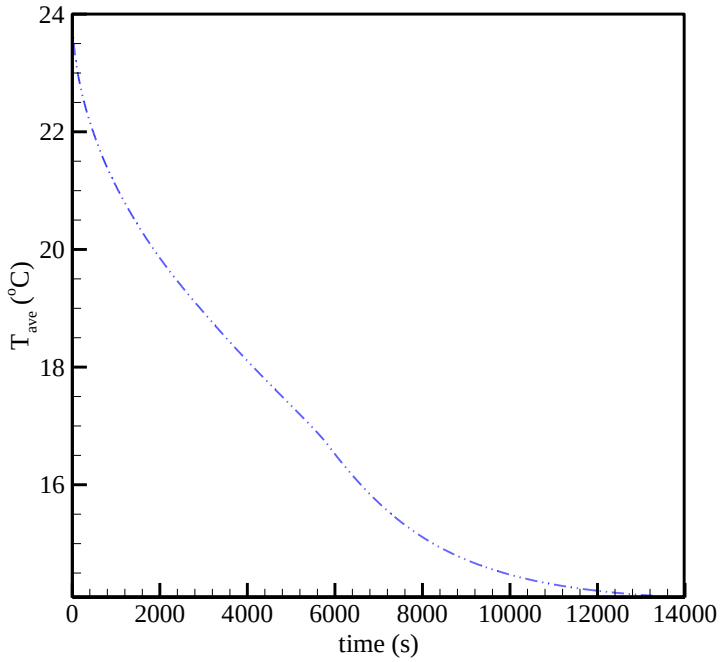

Fig. 4: Temporal variation of the average PCM temperature during the solidification process.

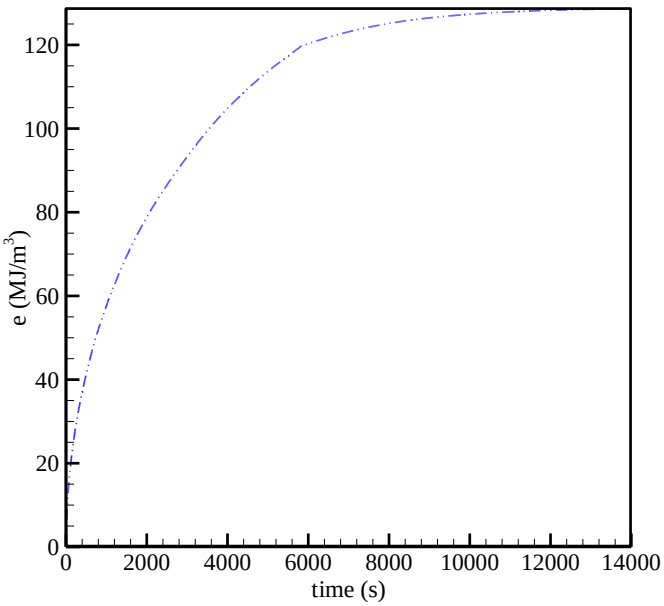

Fig. 6: Temporal variation of energy stored in PCM during the solidification process.

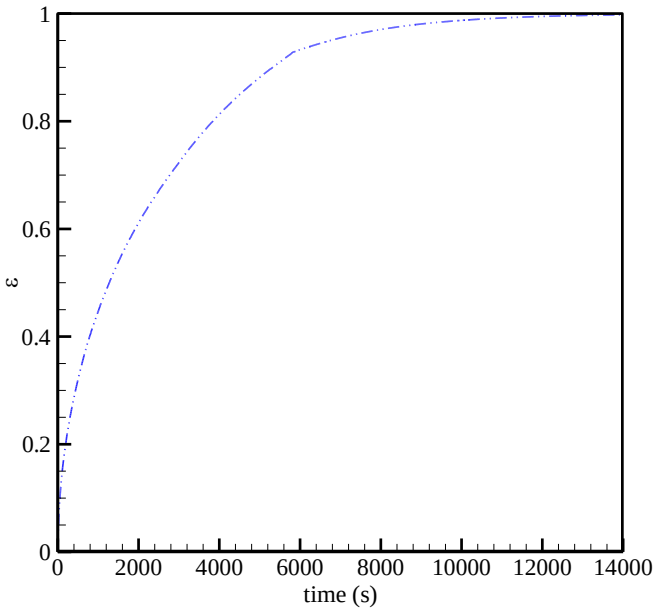

Fig. 7: Temporal variation of the (dimensionless) energy transferred from the liquid PCM to the HTF.

The density of energy released (energy per volume) by the PCM during the solidification process is depicted in Fig. 4. As can be seen, the released energy continuously increases until it achieves the maximum value of 128.7 MJ/m^3 (e_m). It is also interesting to report the variation of released energy as a fraction of maximum thermal energy that the system is capable of releasing at the end of discharging process $\varepsilon = E/E_m$; where E_m is calculated by:

$$E_m = \forall_{PCM}\left[c_{p,l}\rho_l\left(T_0 - T_m\right) + \left(\frac{\rho_s + \rho_l}{2}\right)h_{sf} + c_{p,s}\rho_s\left(T_m - T_c\right)\right] \qquad 11)$$

Figure 5 shows the dimensionless released energy profiles; ε versus time. As seen, the trend is similar to the SF profile shown in Fig.3.

4. Conclusion

In this paper, the novel latent heat exchanger using a toroidal tube was numerically studied through the simulation of phase change heat transfer during solidification of PCM inside the LHTES system. A mathematical model based on the enthalpy-porosity approach was developed and numerically solved by finite volume method to simulate the energy transport processes inside the system. The progression of the solidification was numerically visualized to track the phase change interface at different stages of the process. Several transient heat transfer characteristics, e.g., solid fraction, and released energy storage, during phase change, were determined to investigate phase change patterns and also to evaluate the thermal performance of the system. The findings of the present study can be useful to researchers and engineers in designing efficient latent heat exchangers.

Acknowledgments

The authors sincerely acknowledge the financial aid provided by Discovery Grant from NSERC (Natural Sciences and Engineering Research Council) Canada

References

[1] H. Nazir, M. Batool, F. J. Bolivar Osorio, M. Isaza-Ruiz, X. Xu, K. Vignarooban, P. Phelan, Inamuddin, A. M. Kannan, "Recent developments in phase change materials for energy storage applications: A review," *International Journal of Heat and Mass Transfer*, vol. 129, pp. 491-523, 2019/02/01/ 2019.

[2] O. Behar, A. Khellaf, and K. Mohammedi, "A review of studies on central receiver solar thermal power plants," *Renewable and sustainable energy reviews*, vol. 23, pp. 12-39, 2013.

[3] M. Mohaghegh, "Nanofluids Applications in Solar Energy Systems: A Review," *Journal of Solar Energy Research*, vol. 3, pp. 57-65, 2018.

[4] K. Ghasemi, S. Tasnim, and S. Mahmud, "PCM, nano/microencapsulation and slurries: A review of fundamentals, categories, fabrication, numerical models and applications," *Sustainable Energy Technologies and Assessments*, vol. 52, p. 102084, 2022.

[5] K. Ghasemi, S. Tasnim, and S. Mahmud, "Shape-stabilized phase change material convective melting by considering porous configuration effects," *Journal of Molecular Liquids*, p. 118956, 2022.

[6] M. R. Mohaghegh, Y. Alomair, M. Alomair, S. H. Tasnim, S. Mahmud, and H. Abdullah, "Melting of PCM inside a novel encapsulation design for thermal energy storage system," *Energy Conversion and Management: X*, vol. 11, p. 100098, 2021/09/01/ 2021.

[7] Z. Hu, A. Li, R. Gao, and H. Yin, "Enhanced heat transfer for PCM melting in the frustum-shaped unit with multiple PCMs," *Journal of Thermal Analysis and Calorimetry*, vol. 120, pp. 1407-1416, 2015.

[8] A. Sharma, V. V. Tyagi, C. Chen, and D. Buddhi, "Review on thermal energy storage with phase change materials and applications," *Renewable and Sustainable energy reviews*, vol. 13, pp. 318-345, 2009.

[9] M. R. Mohaghegh, S. Mahmud, and S. Tasnim, "Effect of Geometric Configurations on the Thermal Performance Of Encapsulated PCMs," in *ASME 2021 Heat Transfer Summer Conference collocated with the ASME 2021 15th International Conference on Energy Sustainability*, 2021.

[10] S. Patel, S. H. Tasnim, and S. Mahmud, "Phase Change Process inside Toroidal Tube Heat Exchanger with Internal Fins," *Journal of Energy Storage*, p. 103695, 2021.

[11] S. Borhani, M. Hosseini, A. Ranjbar, and R. Bahrampoury, "Investigation of phase change in a spiral-fin heat exchanger," *Applied Mathematical Modelling*, vol. 67, pp. 297-314, 2019.

[12] M. Rahimi, S. S. Ardahaie, M. Hosseini, and M. Gorzin, "Energy and exergy analysis of an experimentally examined latent heat thermal energy storage system," *Renewable Energy*, vol. 147, pp. 1845-1860, 2020.

[13] S. S. Ardahaie, M. Hosseini, A. Ranjbar, and M. Rahimi, "Energy storage in latent heat storage of a solar thermal system using a novel flat spiral tube heat exchanger," *Applied Thermal Engineering*, vol. 159, p. 113900, 2019.

[14] M. Alomair, Y. Alomair, S. Tasnim, S. Mahmud, and H. Abdullah, "Analyses of Bio-Based Nano-PCM filled Concentric Cylindrical Energy Storage System in Vertical Orientation," *Journal of Energy Storage*, vol. 20, pp. 380-394, 2018/12/01/ 2018.

[15] S. Kahwaji and M. A. White, "Edible oils as practical phase change materials for thermal energy storage," *Applied Sciences*, vol. 9, p. 1627, 2019.

[16] S. Ebadi, S. H. Tasnim, A. A. Aliabadi, and S. Mahmud, "Melting of nano-PCM inside a cylindrical thermal energy storage system: Numerical study with experimental verification," *Energy Conversion and Management*, vol. 166, pp. 241-259, 2018/06/15/ 2018.

[17] V. R. Voller and C. Prakash, "A fixed grid numerical modelling methodology for convection-diffusion mushy region phase-change problems," *International Journal of Heat and Mass Transfer*, vol. 30, pp. 1709-1719, 1987.

[18] A. Brent, V. R. Voller, and K. Reid, "Enthalpy-porosity technique for modeling convection-diffusion phase change: application to the melting of a pure metal," *Numerical Heat Transfer, Part A Applications*, vol. 13, pp. 297-318, 1988.